TECHNICAL REPORT STANDARD PAGE

1. Report No.	2. Government Accession No.	3. Recipient's Catalog No.
FHWA/LA-92/256		

4. Title and Subtitle	5. Report Date
TRAFFIC ACCIDENT SIMULATION	June 1992
	6. Performing Organization Code 256

7. Author(s)	8. Performing Organization Report No.
John E. Beard, Ph.D.	256

9. Performing Organization Name and Address	10. Work Unit No.
Department of Mechanical Engineering Louisiana State University Baton Rouge, LA 70803	11. Contract or Grant No. LA HPR NO. 89-1SS(B)

12. Sponsoring Agency Name and Address	13. Type of Report and Period Covered
Louisiana Transportation Research Center 4101 Gourrier Avenue Baton Rouge, LA 70808	Final Report
	14. Sponsoring Agency Code

15. Supplementary Notes

Conducted in cooperation with the U.S. Department of Transportation, Federal Highway Administration.

16. Abstract

The purpose of this research was to determine if HVOSM (Highway Vehicle Object Simulation Model) could be used to model a vehicle with a modern front (or rear) suspension system such as a McPherson strut and have the results of the dynamic model be valid. To accomplish this task, the types of suspension systems modeled in HVOSM and how they were mathematically represented in the equations of motion that govern the dynamics of the vehicle in the simulation were investigated.

HVOSM constrains the motion of the center of the wheel to translate along a straight line that is perpendicular to the *X - Y* plane of the coordinate system attached to the vehicle (SAE Standard Coordinates). Tire forces, shock forces, spring forces, anti-pitch and anti-roll forces are calculated and applied to the body of the vehicle. Tire forces caused by the deviation from the straight line motion of the center of the wheel that are a result of the actual geometry of the suspension system are experimentally measured and included in the appropriate body forces.

To determine if a vehicle with a McPherson strut could be accurately modeled in HVOSM, both the McPherson strut and the double a-arm suspension were evaluated kinematically. How each system influenced the change in track width and camber angle through the vertical motion of wheel were compared.

It was determined that a wheel on a vehicle with a McPherson strut suspension system has a "straighter" straight line motion than does a wheel on a vehicle with a double a-arm suspension system.

The results of the study enable the user of HVOSM to model a vehicle with a McPherson strut suspension system and be confident that the simulation is as accurate as if the vehicle had a double a-arm suspension system.

17. Key Words	18. Distribution Statement
Accident Simulation, Suspension Systems	Unrestricted. This document is available to be public through the National Technical Information Service, Springfield, VA 22161.

19. Security Classif. (of this report)	20. Security Classif. (of this page)	21. No. of Pages	22. Price
Unclassified	Unclassified	38	

Form DOT F1700.7 (1-92)

TRAFFIC ACCIDENT SIMULATION

FINAL REPORT

by

JAMES E. BEARD, PH.D.
DEPARTMENT OF MECHANICAL ENGINEERING
CEBA BUILDING
LOUISIANA STATE UNIVERSITY
BATON ROUGE, LA 70803

STATE PROJECT NO. 736-13-0069

LTRC RESEARCH PROJECT NO. 89-1SS(B)

RESEARCH REPORT NO. 256

Conducted by

LOUISIANA DEPARTMENT OF TRANSPORTATION
AND DEVELOPMENT
Louisiana Transportation Research Center
In Cooperation with
U. S. Department of Transportation
FEDERAL HIGHWAY ADMINISTRATION

JUNE 1992

ACKNOWLEDGEMENTS

Funding for this research was provided by the Louisiana Transportation Research Center (LTRC).

The author appreciates the cordial working relationship generated by Mr. Ara Aram, P.E., Mr. William Temple, P.E., Mr. William King, P.E., and Mr. Steve Cumbaa, P.E. Special thanks are given to Mr. Cumbaa for his extraordinary effort in administrating this project to its completion.

The author also gratefully acknowledges the effort of Dr. Warren N. Waggenspack, Jr. of the Department of Mechanical Engineering, Louisiana State University, for providing much needed assistance at the conclusion of the research project.

The author also thanks Chan Soo Kim, the Graduate Research Assistant on the project.

ABSTRACT

The purpose of this research was to determine if HVOSM (Highway Vehicle Object Simulation Model) could be used to model a vehicle with a modern front (or rear) suspension system such as a McPherson strut and have the results of the dynamic model be valid. To accomplish this task, the types of suspension systems modeled in HVOSM and how they were mathematically represented in the equations of motion that govern the dynamics of the vehicle in the simulation were investigated.

HVOSM constrains the motion of the center of the wheel to translate along a straight line that is perpendicular to the $X - Y$ plane of the coordinate system attached to the vehicle (SAE Standard Coordinates). Tire forces, shock forces, spring forces, anti-pitch and anti-roll forces are calculated and applied to the body of the vehicle. Tire forces caused by the deviation from the straight line motion of the center of the wheel that are a result of the actual geometry of the suspension system are experimentally measured and included in the appropriate body forces.

To determine if a vehicle with a McPherson strut could be accurately modeled in HVOSM, both the McPherson strut and the double a-arm suspension were evaluated kinematically. How each system influenced the change in track width and camber angle through the vertical motion of wheel were compared.

It was determined that a wheel on a vehicle with a McPherson strut suspension system has a "straighter" straight line motion than does a wheel on a vehicle with a double a-arm suspension system.

The results of the study enable the user of HVOSM to model a vehicle with a McPherson strut suspension system and be confident that the simulation is as accurate as if the vehicle had a double a-arm suspension system.

IMPLEMENTATION STATEMENT

The results of this research have verified that HVOSM may be used in predicting the dynamic response of a vehicle if that vehicle has the following suspension systems.

- an independent suspension system on all four wheels
- an independent suspension system on the front wheels and beam type suspension system on the rear
- a beam type suspension system on both the front and rear
- a beam type suspension system on the front and independent suspension system on the rear
- a McPherson strut suspension system on the front and a beam type suspension systems on the rear
- a McPherson strut suspension system on the front and an independent type suspension systems on the rear
- a McPherson strut suspension system on the front and rear

To implement the results requires the same vehicle parameters as presently needed for the double a-arm type suspension systems.

Contents

List of Tables

List of Figures

INTRODUCTION

In an effort to quantify the parameters causing and/or influencing a traffic accident, various computer simulation models have been developed by researchers in the past thirty years. Computer simulation models such as CRASH, EDCRASH, HVOSM, IMPAC, SMAC, VDANL, etc. have various levels of vehicle representation. They range from a vehicle represented as a rigid body with three degrees of freedom without provision for a suspension system to a vehicle represented by a rigid body with eleven degrees-of-freedom and a complete suspension system. Several simulation packages include energy dissipation from collisions of the vehicle with road side barriers or other vehicles. The simulation results may be used to identify road hazards, dangereous traffic patterns, areas of liability for an accident and to determine the vehicle speeds and conditions prior to an accident. Of the simulation packages considered by Louisiana Tech, HVOSM is the software used to determine the vehicle trajectory. It was selected because "source FORTRAN 4 code, extensive documation and public comment in the open literature were available." as stated in Anderson (1991).

OBJECTIVES

The objectives of this study include:

[1] The implementation a of "Traffic Accident Reconstruction" simulation code with interactive computer graphics at LSU that may be utilized by researchers at LTRC. The researchers at Louisiana Tech have provided the graphics code to represent the output (from existing simulation packages) in a manner that may be viewed on a graphics screen. The x,y,z, roll, pitch and yaw values of the moving vehicle used in the generation of the graphics representation are obtained from the Highway Vehicle Object Simulation Model (HVOSM) reconstruction software.

[2] The decoupling of the suspension system model in HVOSM to determine how tire reaction forces resulting from the suspension system geometry are transmitted to the sprung mass. The decoupling will be used to determine if a McPherson strut suspension system can be as accurately represented in HVOSM as the double a-arm or solid beam suspension system is presently modeled in HVOSM.

SCOPE

It was initially determined that we would assist La Tech in evaluating the interactive computer graphics software package. We would also assist researchers at LTRC in preparing the reconstruction of a particular accident and would provide a local source of reconstruction expertise.

The major portion of the project addresses the validity of using HVOSM to simulate modern vehicle suspension systems. The simulation package HVOSM was developed prior to the widespread use of McPherson Strut suspension systems and was only validated for double a-arms and solid beam type suspension systems. This portion is not intended to replace existing simulation packages, but to determine if HVOSM is valid for use in reconstruction when the vehicle in question has a McPherson strut suspension system.

METHODOLOGY

The methodology used is to determine what method is used in HVOSM to mathematically model the kinematics of the suspension system and how the influence of the suspension

system kinematics (geometry) on the displacement of the wheel relative to the unsprung mass (vehicle body) is represented mathematically. The displacment of the wheel directly influences the interaction between the tire and the road and thus the reaction forces on the sprung mass. Once the mathematical model used in HVOSM is determined, it can be compared to the kinematics of the double a-arm and the McPherson strut.

SUSPENSION SYSTEM KINEMATICS

The authors of HVOSM have validated the use of a planar four-link mechanism to simulate the four-link mechanism shown in Figure 1. This mechanism is a subset of the front suspension system. The front suspension system typicially consists of upper and lower a-arms, spindle, anti-sway bar, etc. The upper and lower a-arms, the spindle (often referred to as the "king pin" or "king pin assembly") and frame have the kinematic classification as a revolute-spherical-spherical-revolute (RSSR) mechanism by virtue of the revolute joint at P_1, the spherical joint at P_4, the spherical joint at P_3 and the revolute joint at P_2. Revolute joints connect both the upper and lower a-arms to the vehicle frame. The spherical joints at P_3 and P_4 connect the coupler link to the upper and lower a-arms. The axle is rigidly attached to the coupler link. The spherical joints allow the axle rotation to effect the turning motion of the vehicle, however they do *not* influence the relative rotation of the coupler link for a given position of the a-arms. This means that for a given angular position of the upper and lower a-arm, the coupler link may rotate about the axis defined by the vector r_{KP} in Figure 1. This rotation allows an infinity of solutions of the orientation of the coupler about the line segement r_{KP} without movement of the upper and lower a-arms

The authors of HVOSM also validated the replacement of the planar four-bar with a sprung mass that translates along a straight line, see Figure 2. A further restriction placed on the model is that constraints on the suspension system preclude motion of the unsprung masses in the X and Y direction (relative to the moving coordinate system). This restriction of the planar wheel movement now restricts the movement to be in a plane that is parallel to the $Y - Z$ axis of the vehicle.

Because the double a-arm suspension system has been experimentally validated, the primary goal of this portion of the research is to determine if a McPherson strut suspension system has approximately the same kinematic characteristics relative to the kinematic and dynamic response of the wheel. If so, the McPherson strut may be reduced to the same type of model as the four-link mechanism for accurate simulation without experimental validation.

NOMENCLATURE

The following are the symbols needed for the development of the kinematic relationships for the double a-arm and McPherson strut suspension systems.

r_Z = Distance to center of gravity in the Z direction from the road surface datum.

r_{F1} = Distance to pin joint connecting lower a-arm to the frame.

r_{F2} = Distance from the pin joint connecting the lower a-arm to the frame to the pin joint connecting the upper a-arm to the frame (P_1 to P_2).

r_{LA} = Length of lower a-arm .

r_{UA} = Length of upper a-arm.

r_{KP} = Length of coupler link or connecting link.

r_C = Length of vector from P_4 to the center of the tire.

r_{2Y} = Distance in the Y-direction along the road surface datum to the center of vector r_{2Z}.

r_{2Z} = Distance from the center of the wheel to the road surface datum (*input*).

R_L = r_{2Z}, Distance from the center of the wheel to the road contact (SAE Standards.)

θ_{F1} = Angle of r_{F1} relative to the Y-axis.

θ_{F2} = Angle of r_{F2} relative to the Y-axis.

θ_{LA} = Angle of r_{LA} relative to the Y-axis.

θ_{UA} = Angle of r_{UA} relative to the Y-axis.

θ_{KP} = Angle of r_{KP} relative to the Y-axis.

θ_T = Angle of the wheel axle relative to the Y-axis.

θ_{2Y} = Angle of r_{2Y} relative to the Y-axis.

θ_{2Z} = Angle of r_{2Z} relative to the Y-axis.

θ_Z = Angle of r_Z relative to the Y-axis.

α = Angle between r_{KP} and r_C on the double a-arm.

α_M = Angle between r_S and r_C on the McPherson strut.

S_{2Z_0} = Position of the tire relative to the datum at $X(t) = 0$.
S_{2Z} = Position of the tire relative to the datum.

A_0 = Height of "wave" in the road surface.
λ = Period or wave length of the sinusodial wave in the road.

Nomenclature Specific to the McPherson Strut

r_{F2} = Distance from the pin joint connecting the lower a-arm to the frame to the spherical joint connecting the McPherson strut to the frame (P_1 to P_2).

r_S = Distance along the McPherson strut from P_2 to A.

r_P = Distance from the pin joint connecting the strut assembly to the frame to the lower a-arm to the vector r_S. The vector r_S is perpendicular to r_P.

DEVELOPMENT OF KINEMATIC RELATIONSHIPS

To make a direct comparison between the four-bar and McPherson strut we first examine the kinematic differences. Both mechanisms are oriented such that for a position of a given point on the wheel, the displacement of this point from the road surface (r_{2Z}) is used as the input to the system, see Figure 1. This point is defined as point C and may be set at a value of interest in the simulation software package *KINEMATIC*. The variables of primary interest are r_{2Y} and θ_T. Figure 4 shows θ_t. To determine the value of these variables, a vector loop(s) containing these variables is needed. They are:

$$\text{LOOP I}: \ \overline{r}_Z + \overline{r}_{F1} + \overline{r}_{LA} + \overline{r}_C - \overline{r}_{2Z} - \overline{r}_{2Y} = 0 \tag{1}$$

The angle θ_T is not in Loop I, but is related to θ_{KP} by a constant as shown in Figure 1. Because this is a planar vector loop, two equations are present. In this set of equa-

tions θ_{LA}, θ_{KP} and r_{2Y} are unknown. Because there are only two equations and three unknowns, additional equations are needed. An additional set of equations are written as:

$$\text{LOOP II}: \ \bar{r}_{LA} + \bar{r}_{KP} - \bar{r}_{UA} - \bar{r}_{F2} = 0 \tag{2}$$

Loop II contains an additional unknown in θ_{UA} and two additional independent equations. By summing components, Equations 1 and 2 are represented as:

$$\begin{aligned}
\sum Y_1 &= r_Z \cos\theta_Z + r_{F1}\cos\theta_{F1} + r_{LA}\cos\theta_{LA} + r_C\cos(\theta_{KP}-\alpha) - r_{2Z}\cos\theta_{2Z} - r_{2Y}\cos\theta_{2Y} = 0 \\
\sum Z_1 &= r_Z \sin\theta_Z + r_{F1}\sin\theta_{F1} + r_{LA}\sin\theta_{LA} + r_C\sin(\theta_{KP}-\alpha) - r_{2Z}\sin\theta_{2Z} - r_{2Y}\sin\theta_{2Y} = 0 \\
\sum Y_2 &= r_{LA}\cos\theta_{LA} + r_{KP}\cos\theta_{KP} - r_{UA}\cos\theta_{UA} - r_{F2}\cos\theta_{F2} = 0 \\
\sum Z_2 &= r_{LA}\sin\theta_{LA} + r_{KP}\sin\theta_{KP} - r_{UA}\sin\theta_{UA} - r_{F2}\sin\theta_{F2} = 0
\end{aligned} \tag{3}$$

Although the four independent scalar equations above contain only four unknowns, θ_{LA}, θ_{KP}, θ_{UA} and r_{2Y}, they are non-linear. The values of θ_{LA}, θ_{KP} and r_{2Y} are determined using a numerical methods scheme. A complete derivation is in Appendix 1.

Once θ_{LA}, θ_{KP}, θ_{UA} and r_{2Y} have been calculated within an allowable tolerance[1] (the position is known) the angular velocity and acceleration of each component are determined. They are determined using the velocity and acceleration of point C in the Z direction as the input coefficients that relate the angular velocity and acceleration of the various components to the velocity and acceleration of point C. The coefficients are classified as the kinematic coefficients (Hall, 1991). Kinematic coefficients are defined as:

$$\begin{aligned}
h_{LA} &= \frac{d\theta_{LA}}{dr_{2Z}}, & h'_{LA} &= \frac{d^2\theta_{LA}}{dr_{2Z}^2} \\
h_{KP} &= \frac{d\theta_{KP}}{dr_{2Z}}, & h'_{KP} &= \frac{d^2\theta_{KP}}{dr_{2Z}^2} \\
h_{UA} &= \frac{d\theta_{UA}}{dr_{2Z}}, & h'_{UA} &= \frac{d^2\theta_{UA}}{dr_{2Z}^2} \\
f_{2Y} &= \frac{dr_{2Y}}{dr_{2Z}}, & f'_{2Y} &= \frac{d^2r_{2Y}}{dr_{2Z}^2}
\end{aligned} \tag{4}$$

Therefore the velocity and acceleration of the suspension links can be written as:

$$\ddot{\theta}_{LA} = h'_{LA}\dot{r}_{2Z}^2 + h_{LA}\ddot{r}_{2Z} \tag{5}$$

[1]The tolerance is 0.001 inches for linear displacement and 0.01° for angular displacement.

$$\ddot{\theta}_{KP} = h'_{KP}\dot{r}^2_{2Z} + h_{KP}\ddot{r}_{2Z} \tag{6}$$

$$\ddot{\theta}_{UA} = h'_{UA}\dot{r}^2_{2Z} + h_{UA}\ddot{r}_{2Z} \tag{7}$$

To solve for the kinematic coefficients we differentiate Equations 3 with respect to the input variable r_{2Z}

$$\begin{Bmatrix} 0 \\ -1 \\ 0 \\ 0 \end{Bmatrix} = \begin{bmatrix} -r_{LA}\sin\theta_{LA} & , -r_C\sin(\theta_{KP}-\alpha) & , 0 & , 1 \\ -r_{LA}\cos\theta_{LA} & , -r_C\cos(\theta_{KP}-\alpha) & , 0 & , 0 \\ -r_{LA}\sin\theta_{LA} & , -r_{KP}\sin\theta_{KP} & , r_{UA}\sin\theta_{UA} & , 0 \\ r_{LA}\cos\theta_{LA} & , r_{KP}\cos\theta_{KP} & , -r_{UA}\cos\theta_{UA} & , 0 \end{bmatrix} \begin{Bmatrix} h_{LA} \\ h_{KP} \\ h_{UA} \\ f_{2Y} \end{Bmatrix} \tag{8}$$

and for the second derivative

$$\begin{Bmatrix} r_{LA}\cos(\theta_{LA})h^2_{LA} + r_C\cos(\theta_{KP}-\alpha)h^2_{KP} \\ r_{LA}\sin(\theta_{LA})h^2_{LA} + r_C\sin(\theta_{KP}-\alpha)h^2_{KP} \\ r_{LA}\cos(\theta_{LA})h^2_{LA} + r_{KP}\cos(\theta_{KP})h^2_{KP} - r_{UA}\cos(\theta_{UA})h^2_{UA} \\ r_{LA}\sin(\theta_{LA})h^2_{LA} + r_{KP}\sin(\theta_{KP})h^2_{KP} - r_{UA}\sin(\theta_{UA})h^2_{UA} \end{Bmatrix} =$$

$$\begin{bmatrix} -r_{LA}\sin\theta_{LA} & , -r_C\sin(\theta_{KP}-\alpha) & , 0 & , 1 \\ -r_{LA}\cos\theta_{LA} & , -r_C\cos(\theta_{KP}-\alpha) & , 0 & , 0 \\ -r_{LA}\sin\theta_{LA} & , -r_{KP}\sin\theta_{KP} & , r_{UA}\sin\theta_{UA} & , 0 \\ r_{LA}\cos\theta_{LA} & , r_{KP}\cos\theta_{KP} & , -r_{UA}\cos\theta_{UA} & , 0 \end{bmatrix} \begin{Bmatrix} h'_{LA} \\ h'_{KP} \\ h'_{UA} \\ f'_{2Y} \end{Bmatrix} \tag{9}$$

Equation 8 is a set of four equations with four unknowns written in matrix form and can be solved using a varity of techniques such as Gauss-elimination, Crammer's rule, etc. Once Equation 8 is solved, the values of h_{LA}, h_{KP}, h_{UA} and f_{2Y} are used to solve Equation 9. It is also a set of four linear equations with four unknowns.

The same techniques used to solve for the position, velocity and acceleration of the double a-arm are now applied to solving for the position, velocity and acceleration of the components of a McPherson strut shown in Figure 3. The vector loops used are:

$$\text{LOOP I}: \ \bar{r}_Z + \bar{r}_{F1} + \bar{r}_{LA} + \bar{r}_C - \bar{r}_{2Z} - \bar{r}_{2Y} = 0 \tag{10}$$

The second loop is

$$\text{LOOP II}: \ \bar{r}_{LA} + \bar{r}_P + \bar{r}_S - \bar{r}_{F2} = 0 \tag{11}$$

Both loops are needed to solve for the variables r_{2Y} and θ_T using r_{2Z} as the input. By summing components, Equations 10 and 11 are represented as:

$$\begin{aligned}
\sum Y_1 &= r_Z \cos\theta_Z + r_{F1}\cos\theta_{F1} + r_{LA}\cos\theta_{LA} + r_C\cos(\theta_S-\alpha) - r_{2Z}\cos\theta_{2Z} - r_{2Y}\cos\theta_{2Y} = 0 \\
\sum Z_1 &= r_Z \sin\theta_Z + r_{F1}\sin\theta_{F1} + r_{LA}\sin\theta_{LA} + r_C\sin(\theta_S-\alpha) - r_{2Z}\sin\theta_{2Z} - r_{2Y}\sin\theta_{2Y} = 0 \\
\sum Y_2 &= r_{LA}\cos\theta_{LA} + r_P\cos(\theta_S-90) + r_S\cos\theta_S - r_{F2}\cos\theta_{F2} = 0 \\
\sum Z_2 &= r_{LA}\sin\theta_{LA} + r_K P\sin(\theta_S-90) + r_S\sin\theta_S - r_{F2}\sin\theta_{F2} = 0
\end{aligned} \tag{12}$$

The values of θ_{LA}, θ_S, r_S and r_{2Y} are determined using the same numerical method technique employed to solve the position equations of the double a-arm. A complete derivation is given in Appendix 1.

Once θ_{LA}, θ_S, r_S and r_{2Y} have been calculated within an allowable tolerence [2] (the position is known) the velocity and acceleration of each component are determined. They are determined using the velocity and acceleration of point C in the Z direction and kinematic coefficients. Kinematic coefficients for these loops are defined as follows:

$$\begin{aligned}
h_{LA} &= \frac{d\theta_{LA}}{dr_{2Z}}, & h'_{LA} &= \frac{d^2\theta_{LA}}{dr_{2Z}^2} \\
h_S &= \frac{d\theta_S}{dr_{2Z}}, & h'_S &= \frac{d^2\theta_S}{dr_{2Z}^2} \\
f_S &= \frac{dr_S}{dr_{2Z}}, & f'_S &= \frac{d^2 r_S}{dr_{2Z}^2} \\
f_{2Y} &= \frac{dr_{2Y}}{dr_{2Z}}, & f'_{2Y} &= \frac{d^2 r_{2Y}}{dr_{2Z}^2}
\end{aligned} \tag{13}$$

Differentiating Equations 12 with respect to the input variable r_{2Z}

$$\begin{Bmatrix} 0 \\ -1 \\ 0 \\ 0 \end{Bmatrix} = \begin{bmatrix} -r_{LA}\sin\theta_{LA} & , -r_C\sin(\theta_S-\alpha) & , 0 & , 1 \\ -r_{LA}\cos\theta_{LA} & , -r_C\cos(\theta_S-\alpha) & , 0 & , 0 \\ -r_{LA}\sin\theta_{LA} & , -r_P\sin(\theta_S-90) - r_S\sin\theta_S & , \cos\theta_S & , 0 \\ r_{LA}\cos\theta_{LA} & , r_P\cos(\theta_S-90) - r_S\cos\theta_S & , \sin\theta_S & , 0 \end{bmatrix} \begin{Bmatrix} h_{LA} \\ h_S \\ f_S \\ f_{2Y} \end{Bmatrix} \tag{14}$$

and for the second derivative

$$\begin{Bmatrix} r_{LA}\cos(\theta_{LA})h_{LA}^2 + r_C\cos(\theta_S-\alpha)h_S^2 \\ r_{LA}\sin(\theta_{LA})h_{LA}^2 + r_C\sin(\theta_S-\alpha)h_S^2 \\ r_{LA}\cos(\theta_{LA})h_{LA}^2 + r_P\cos(\theta_S-90)h_S^2 + r_S\cos(\theta_S)h_S^2 + 2f_S h_S\sin\theta_S \\ r_{LA}\sin(\theta_{LA})h_{LA}^2 + r_P\sin(\theta_S-90)h_S^2 + r_S\sin(\theta_S)h_S^2 - 2f_S h_S\cos\theta_S \end{Bmatrix} =$$

[2] The tolerance is 0.001 inches for linear displacement and 0.01° for angular displacement.

$$\begin{bmatrix} -r_{LA}\sin\theta_{LA} & , -r_C\sin(\theta_S-\alpha) & , 0 & , 1 \\ -r_{LA}\cos\theta_{LA} & , -r_C\cos(\theta_S-\alpha) & , 0 & , 0 \\ -r_{LA}\sin\theta_{LA} & , -r_P\sin(\theta_S-90)-r_S\sin\theta_S & , \cos\theta_S & , 0 \\ r_{LA}\cos\theta_{LA} & , r_P\cos(\theta_S-90)-r_S\cos\theta_S & , \sin\theta_S & , 0 \end{bmatrix} \begin{Bmatrix} h'_{LA} \\ h'_S \\ f'_S \\ f'_{2Y} \end{Bmatrix} \tag{15}$$

Equations 3-15 are used to evaluate the position, velocity and acceleration of the suspension system members.

By comparing the values of the variables r_{2Y}, f_{2Y}, f'_{2Y}, θ_T, h_T and h'_T the comparison will be made between the double a-arm and the McPherson strut.

DISCUSSION OF RESULTS

To illustrate the validity of the representation of the four-bar suspension system as a constrained simple mass-spring damper we examine the variables r_{2Y} and θ_T. As noted earlier, the variable r_{2Y} defines the center of the wheel relative to the center of gravity of the vehicle in the Y direction and θ_T defines the angle of the wheel axle relative to the vehicle in the $Y-Z$ plane. For the double a-arm and McPherson strut the angle of the spindle, θ_T, is defined respectively as:

$\theta_T = \theta_{KP} - \beta$ or $\theta_{\mathrm{T}} = \theta_{\mathrm{S}} - \beta_{\mathrm{M}}$

As shown in Figure 4 the tire foot print is a function of ΔT_{2Z}, Δr_{2Y} and $\Delta\theta_T$. The tire reaction forces are a function of the foot print, therefore the reaction forces applied to the Euler equations that define the motion of the vehicle in HVOSM, are functions of ΔT_{2Y_z}, Δr_{2Y} and $\Delta\theta_T$.

As noted in the methodology section the comparison between the double a-arm and the McPherson strut system will be made by comparing the variables r_{2Y}, f_{2Y}, f'_{2Y}, θ_T, h_T and h'_T for a given position of the center of the tire (other positions on the tire can be analyzed by specifying the appropriate r_C and α values). To make a direct comparison between vehicles that have a different track width or tire size, and thus a different r_{2Z} at the equilibrium position, the value of r_{2Z} plotted on the abssica is Δr_{2Z}. This is where $\Delta r_{2Z} = r_{2Z} - r_{2Z\ @equilibrium}$. The values of $\Delta\theta_T$ and Δr_{2Y} are also plotted where they are $\Delta\theta_T = \theta_T - \theta_{T\ @equilibrium}$ and $\Delta r_{2Y} = r_{2Y} - r_{2Y\ @equilibrium}$ respectively. The comparison will be made in the following sequence.

First the linear portion of the analysis will be presented by examining Δr_{2Y}, $\Delta\theta_T$, f_{2Y} and h_T.

Secondly, the non-linear portion of the analysis will be presented. The terms f'_{2Y} and h'_T are only part of the acceleration equations. Both the angular and linear accelerations of interest, $\ddot{r}_{2Y}$ and $\ddot{\theta}_T$ contain terms that are functions of velocity. To make comparisons, velocity and acceleration values of the vector r_{2Z} are needed. In Figure 5, the location of the contact point between the road and the tire measured from the datum is the vector S_{2Z}. The vector S_{2Z} is constrained to the Z direction. The value of S_{2Z} is a function of the position of the vehicle in the X direction. Because the comparison between the suspension systems is based on evaluating Δr_{2Y} and $\Delta\theta_T$, the variable ΔT_{2Y} that describes the compression of the tire that will be considered to be the same for both systems. In addition, the value of r_{2Y} and S_{2Y} only vary by a constant. This means that:

$$\dot{r}_{2Z} = \dot{S}_{2Z} \qquad \text{and} \qquad \ddot{r}_{2Z} = \ddot{S}_{2Z}$$

To determine a specific value of S_{2Z}, $\dot{S}_{2Z}$ and $\ddot{S}_{2Z}$ a function describing the road surface is needed. Given the function the following relationship can be written as:

$$S_{2Z} = f(X(t)) \tag{16}$$

$$\dot{S}_{2Z} = f'(X)\dot{X} \tag{17}$$

$$\ddot{S}_{2Z} = f''(X)\dot{X}^2 + f'(X)\ddot{X} \tag{18}$$

Although there is an infinite variation of road functions, we will do the analysis for a sinusodial road,therefore:

$$S_{2Z} = S_0 + A_0 \sin\left(\frac{X}{\lambda}\right) \tag{19}$$

$$\dot{S}_{2Z} = \left(\frac{\dot{X}}{\lambda}\right) A_0 \cos\left(\frac{X}{\lambda}\right) \tag{20}$$

$$\ddot{S}_{2Z} = -\left(\frac{\dot{X}}{\lambda}\right)^2 A_0 \sin\left(\frac{X}{\lambda}\right) + \left(\frac{\ddot{X}}{\lambda}\right) A_0 \cos\left(\frac{X}{\lambda}\right) \tag{21}$$

Table 1 shows the values of vehicle velocity ($\dot{X}$), wave height (A_0) and wave length used in the analysis.

Case	$\dot{X}$ (Feet/second)	A_0 (Inches)	λ (Feet)
Case 1	44.0	2.5	20.0
Case 2	44.0	2.5	40.0
Case 3	88.0	2.5	20.0
Case 4	88.0	2.5	40.0

Table 1: Various road conditions for the acceleration analysis.

Variable	Double A-Arm	McPherson Strut
r_Z (Inches)	6.25	6.25
r_{2Z} (Inches)	11.0	10.5
r_{F1} (Inches)	11.1	7.11
r_{F2} (Inches)	15.53	28.0
r_{LA} (Inches)	15.00	12.5
r_{KP} (Inches)	18.5	
r_{UA} (Inches)	8.00	
r_C (Inches)	3.00	9.4
r_P (Inches)		4.18
θ_{F1} (°)	180.0	
θ_{F2} (°)	266.0	
α (°)	18.0	68.7
θ_{LA} (°)	186.71	179.49
θ_{KP} (°)	291.16	
θ_{UA} (°)	206.03	
θ_S (°)		276.34
r_S (Inches)		24.05
r_{2Y} (Inches)	25.83	27.94
Track width, front (Inches)	57.0	54.25
Track width, rear (Inches)	57.0	53.0

Table 2: Kinematic variables for planar analysis of the suspension systems.

LINEAR ANALYSIS, POSITION AND VELOCITY

Figures 6-9 are graphs of Δr_{2Y} -h_T for the double a-arm and the McPherson strut versus the input r_{2Z}. The suspension system examples were taken from two vehicles. A 1989 Hyundai Excel and a 1991 Honda Accord. The Hyundai has a McPherson strut suspension system and the Honda has a double a-arm suspension system. The Hyundai and Honda are similar in wheelbase width and suspension system travel, see Table 2.

First examine the position components. Figure 6 presents Δr_{2Y} versus Δr_{2Z}. This may also be referred to as the rate of track change (SAE). The suspension travel was limited to 2.5 inches in the negative Z direction (up) from equilibrium. Note that the McPherson strut has a Δr_{2Y} of -0.25 inches and the double a-arm has a Δr_{2Y} of a -0.67 inches. The McPherson strut has a Δr_{2Y} that is approximately 33 percent of the double a-arm.

Figure 7 presents $\Delta\theta_T$ versus Δr_{2Z}. This may be referred to the change in camber angle (SAE). Note that the McPherson strut has a maximum $\Delta\theta_T$ of 0.25° and the double a-arm has $\Delta\theta_T$ of 3.20°. The McPherson strut has a $\Delta\theta_T$ that is approximately 8 percent of the rotation of the double-a-arm.

For the velocity components, examine the variables f_{2Y} and h_T. They are the coefficients that describe the rate of change of the track width and the rate of change of camber angle respectively.

Figure 11 presents f_{2Y} versus Δr_{2Z}. This may also be referred to as the rate of track change (SAE). Note that the initial values of h_{2Y} for both the McPherson strut and double a-arm are negative. The initial value for the McPherson strut is -0.015 and decreases to -0.175. The initial value of f_{2Y} for the double a-arm is -0.175 and decreases to -0.375. Both the McPherson strut and double a-arm values of f_{2Y} increase in the negative direction (larger absolute values) as Δr_{2Z} increases.

Figure 9 presents h_{KP} and h_S versus Δr_{2Z}. The kinematic coefficient h_{KP} is the rate of change of the king pin angle versus the displacement and h_S is the rate of change of the angle along the vector r_S. The vector r_S defines the length of the shock absorber and spring plus the appropriate constant. The angle of tire θ_T is related to the angle of the king pin θ_{KP} by a constant on the double a-arm. Also, the angle of the tire is related to the angle θ_S by a constant. Therefore, the rate of change of tire, h_T measures the same variable as h_{KP} or h_S. Note that the McPherson strut has an initial value of h_T of 0.005 that decreases to -0.003 and the double a-arm has an initial h_T value of 0.015 that increases to 0.026. The units on this variable are radians/inch. This means the rate of change of camber angle is initally smaller for the McPherson strut than for the double a-arm and it continues to decrease over the entire range of motion while this

variable continues to increase for the double a-arm over the entire range of motion. Also, note that because h_T for the McPherson strut has a negative slope that $\Delta\theta_T$ reaches a maximum value then decreases in the range analyzed, see Figure 7.

ACCELERATION ANALYSIS

To compare the time derivative of the rate of change of the track width ($\ddot{r}_{2Y}$) and time derivative of the rate of change of the rate of change of the camber angle ($\ddot{\theta}_T$) we need to know the profile of the road and the velocity and acceleration of the vehicle. The data for the four cases examined is given in Table 2. For all the cases, the velocity of the vehicle was a constant for that range of Δr_{2Z}. First examine $\ddot{r}_{2Y}$ with $A_0 = 2.5$inches, $\lambda = 20$feet, $\dot{X} = 44$ ft/sec. and $A_0 = 2.5$ inches, $\lambda = 20$ feet, $\dot{X} = 88$ ft/sec., Figure 13 and Figure 15. For both cases, the initial value of $\ddot{r}_{2Y}$ is slightly larger for the McPherson strut than for the double a-arm (< 1 *percent*). The value of $\ddot{r}_{2Y}$ for the double a-arm increases as Δr_{2Z} increases for both the McPherson strut and double a-arm. The maximum value of $\ddot{r}_{2Z}$ of the McPherson strut is ≈ 47 *percent* of that of the double a-arm for all cases. In addition, the maximum acceleration for all cases is 1.5 ft/second^2 which is 0.05 times the acceleration of gravity (0.05 g's). Note that $\ddot{r}_{2Y}$ is the same for both case 1 and case 4, Figures 13 and 16, because the ratio of $\dot{X}/\lambda$ is the same for both and $\ddot{X} = 0.0$.

Next, examine the angular acceleration of the spindle ($\ddot{\theta}_T$) for the cases of $A_0 = 2.5$inches, $\lambda = 20$ feet, $\dot{X} = 44$ ft/sec. and $A_0 = 2.5$ inches, $\lambda = 20$ feet, $\dot{X} = 88$ ft/sec., Figure 17 and Figure 20. The initial acceleration of the spindle for the McPherson strut is less than that of the double a-arm and remains less until $\Delta r_{2Z} > 1.8$ inches. At the maximum Δr_{2Z}, the McPherson strut has a spindle accleration that is increasing rapidly while the spindle acceleration of the double a-arm is decreasing, however, the magnitude of acceleration is still small, less than 0.035 radians/second^2. Also note that $\ddot{\theta}_T$ is the same for both case 1 and case 4, Figures 17 and 19, because the ratio of $\dot{X}/\lambda$ is the same for both and $\ddot{X} = 0.0$.

Using the previously discussed figures, the application of these results will be discussed in the conclusions.

CONCLUSIONS

The original purpose of the research was to determine if HVOSM could be used to predict dynamic vehicle behavior for a vehicle with a "modern" front suspension system such as

a McPherson strut. To make this decision, first remember that HVOSM constrains the center of the front wheels of an independent suspension system such as a double a-arm to translate along a straight line. They also constrain the plane of the wheel to have zero projection onto the $X - Y$ plane of the coordinate system *on the vehicle* throughout the motion of the wheel. This means the authors of HVOSM assume that regardless of the front suspension system geometry, deviation from straight line motion of the wheel can either be ignored or they have a method to compensate for the deviation. They have chosen to include the additional forces caused by the non-linearities of the system in a "look-up" table. Because the analysis is based on an "adjusted" straight line motion, if the McPherson strut has motion of the wheel center that is as "straight" as the double a-arm, then it follows that it can be represented in HVOSM and the results be acceptable.

From the discusion of the results and Figures 6 to 19 it can be seen that the McPherson strut has "straighter" straight line motion than does the double a-arm. Both the change of track width and the change of camber angle for the McPherson strut over the entire motion is less than that of the double a-arm. This *does not* mean that a vehicle with a McPherson strut will ride or handle better than one with a double a-arm suspension system. It simply means that the McPherson strut suspension system fits the original assumptions used by the authors of HVOSM better than the double a-arm. It follows that because the constraints of straight line motion have been experimentally validated in HVOSM for the double a-arm and that the motion of the wheel of a vehicle with a McPherson strut translates along a straighter line than a double a-arm that a model of a vehicle with a McPherson strut can be represented in HVOSM. This can be accomplished with no additional loss of accuracy in the simulation. In conclusion, HVOSM *can be* used for vehicle dynamic simulation for a vehicle with a McPherson strut suspension system.

RECOMMENDATIONS

It is recommended that a test case involving a vehicle with a McPherson strut suspension system be modeled in HVOSM. The non-linearity of the motion of the center of the front wheel, the spring rate, the shock absorber rate, etc. will have to be measured experimentally, as they would for the double a-arm case. This test case, along with the computer graphics animation of the simulated accident, would enable the legal section of LDOT to determine future research goals in the area of accident simulation.

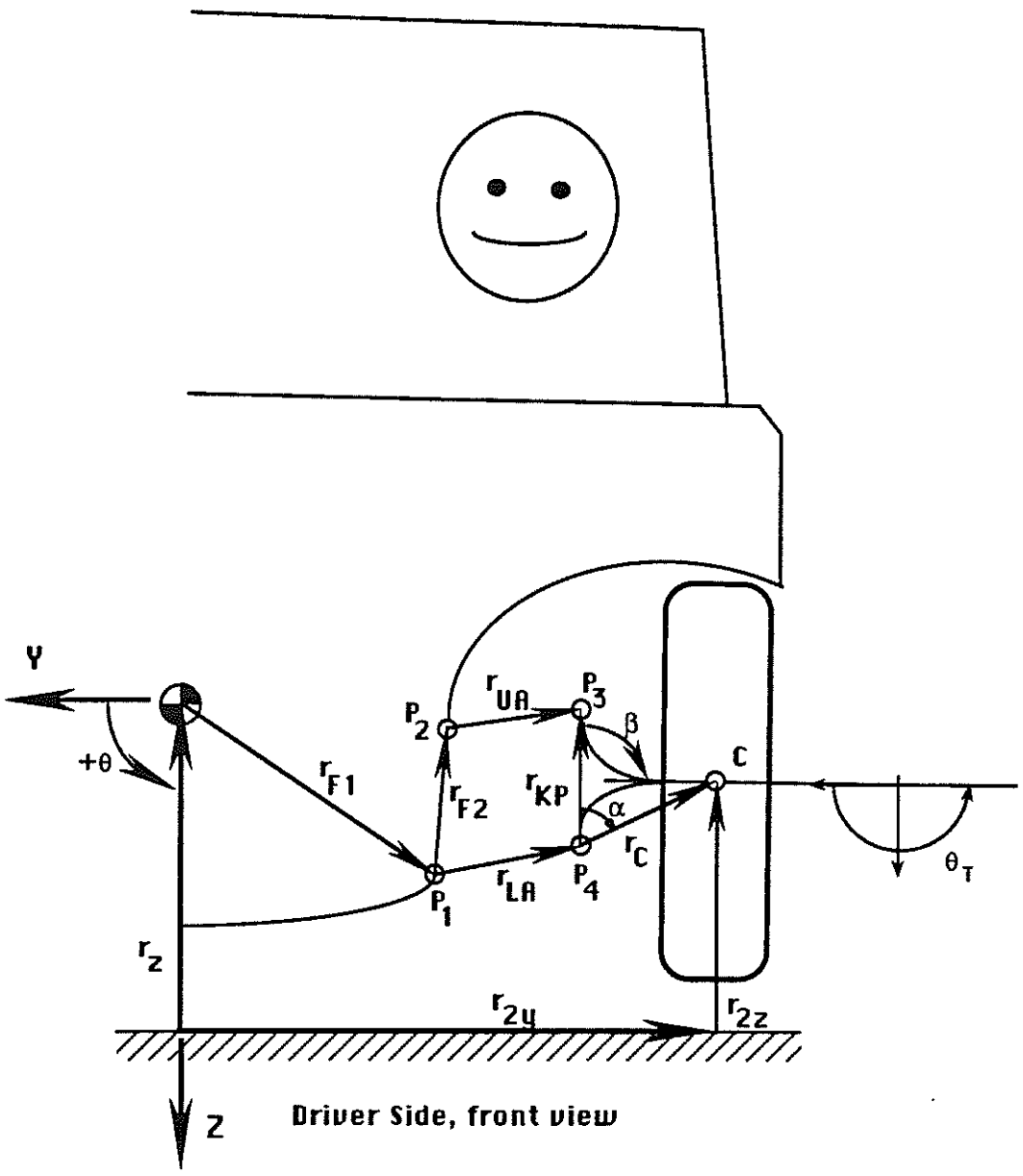

Figure 1: The model of the double a-arm suspension system (Four-bar) and the vectors used to define the location and orientation of the link members.

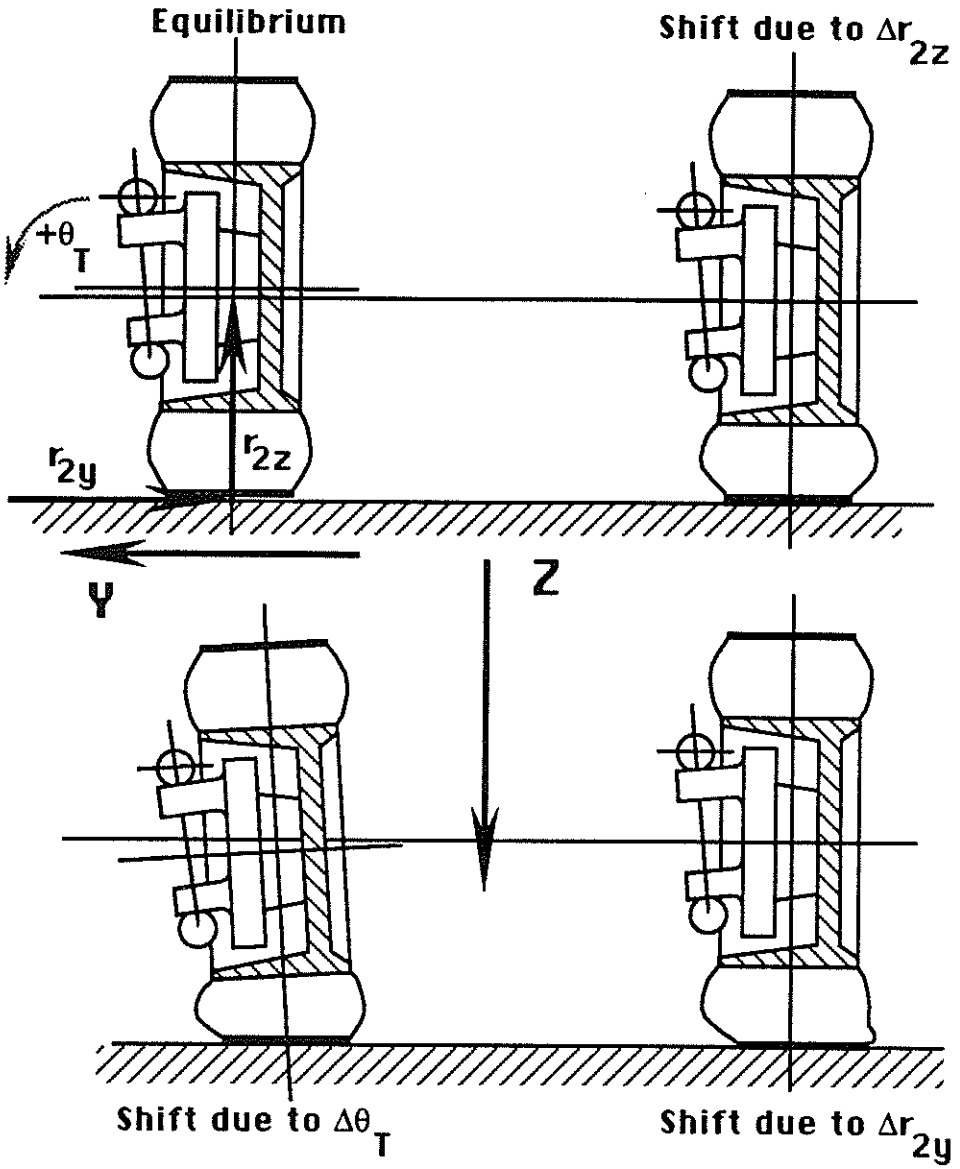

Figure 4: The influence of the variables ΔT_{2Z}, Δr_{2Y} and $\Delta\theta_T$ on the tire foot patch.

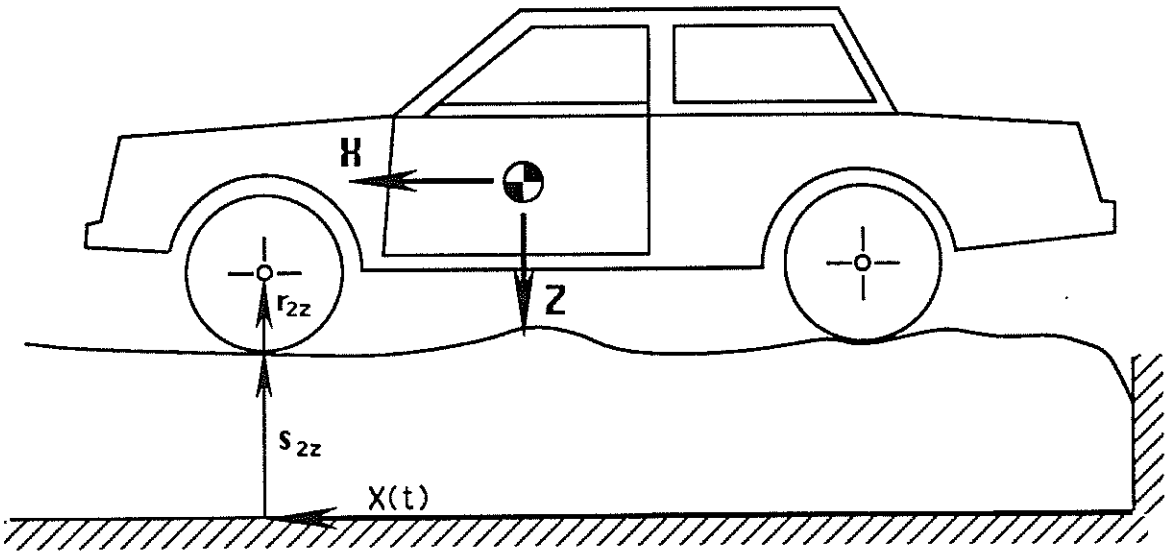

Figure 5: The surface of the road as a function of the vehicles's X displacement.

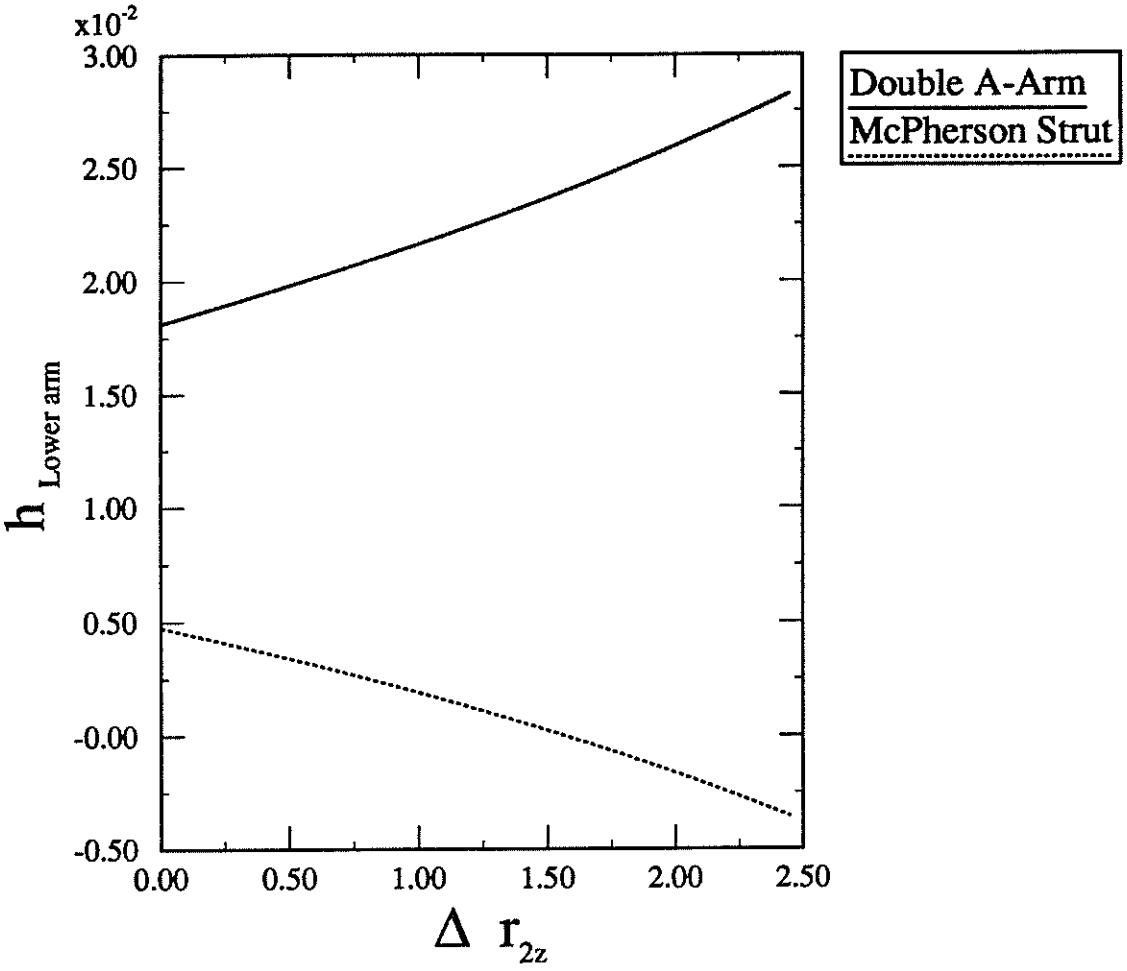

Figure 8: The first order kinematic coefficient h_{LA} versus the relative displacement in the Z-direction, Δr_{2Z}.

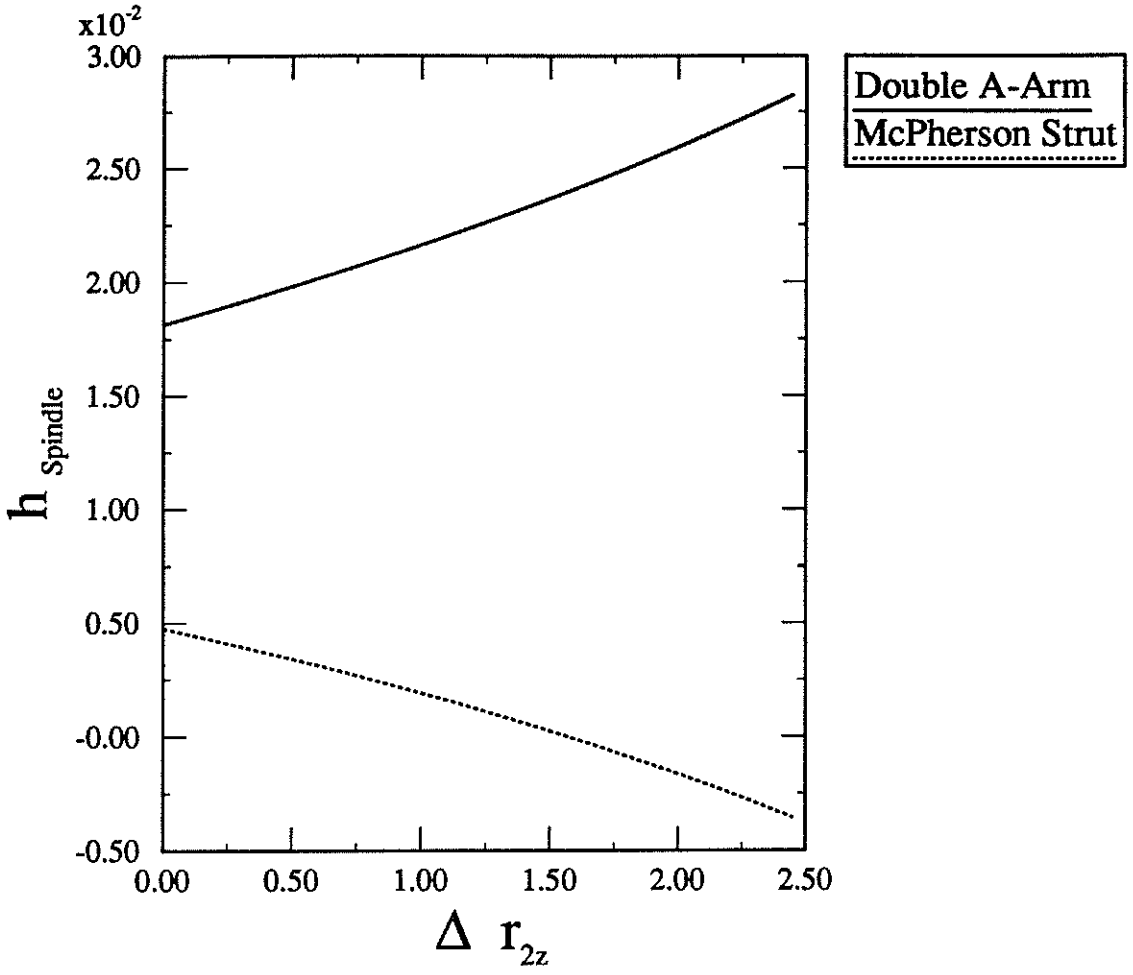

Figure 9: The first order kinematic coefficient h_{KP} and h_S (McPherson Strut) for the coupler link versus the relative displacement in the Z-direction, Δr_{2Z}. The wheel axle is rigidly attached to the coupler link on both the double a-arm and the McPherson strut.

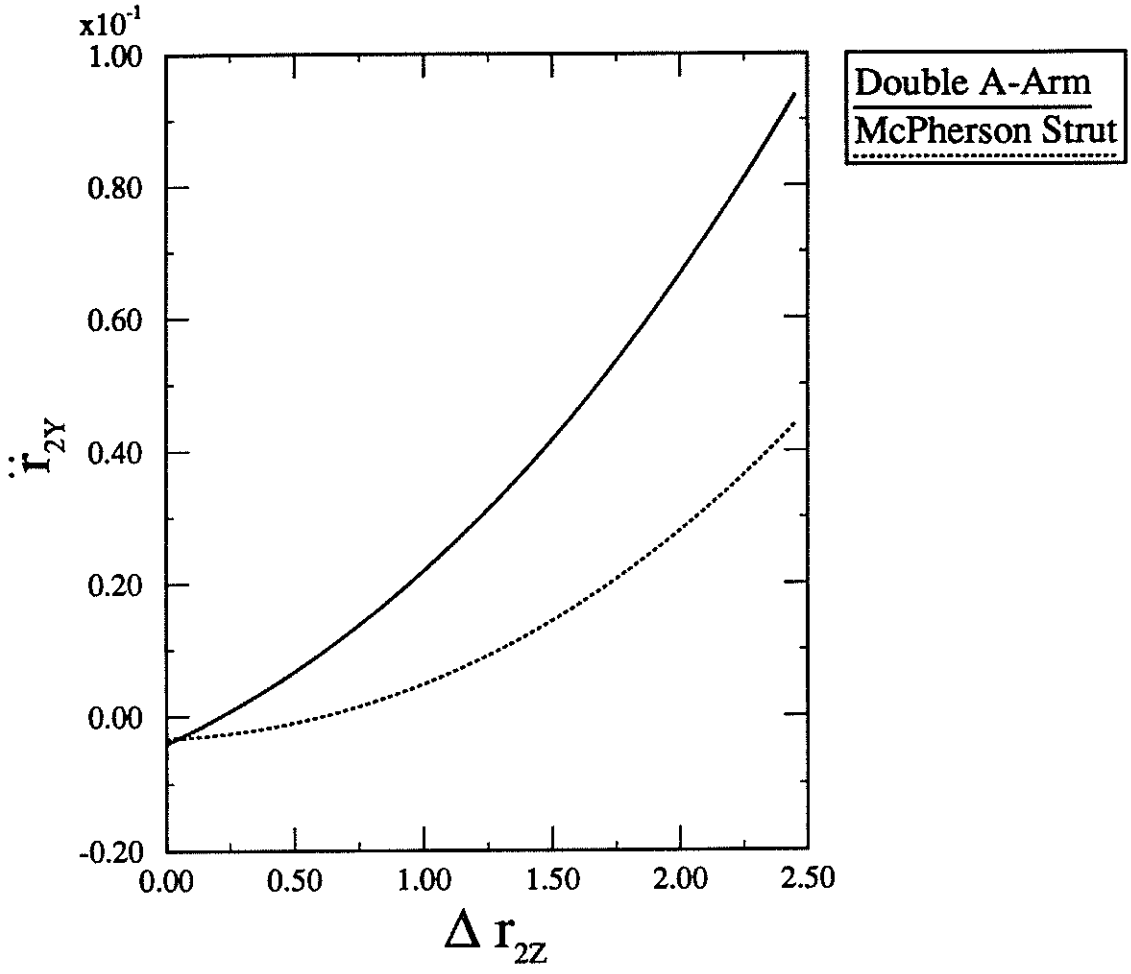

Figure 14: The linear acceleration of the tire contact point, $\ddot{r}_{2Y}$ versus the relative displacement in the Z-direction. The road is sinusodial with $A_0 = 2.5$ inches, $\lambda = 40$ feet, $\dot{X} = 44$ ft/sec. and $\ddot{X} = 0.0$.

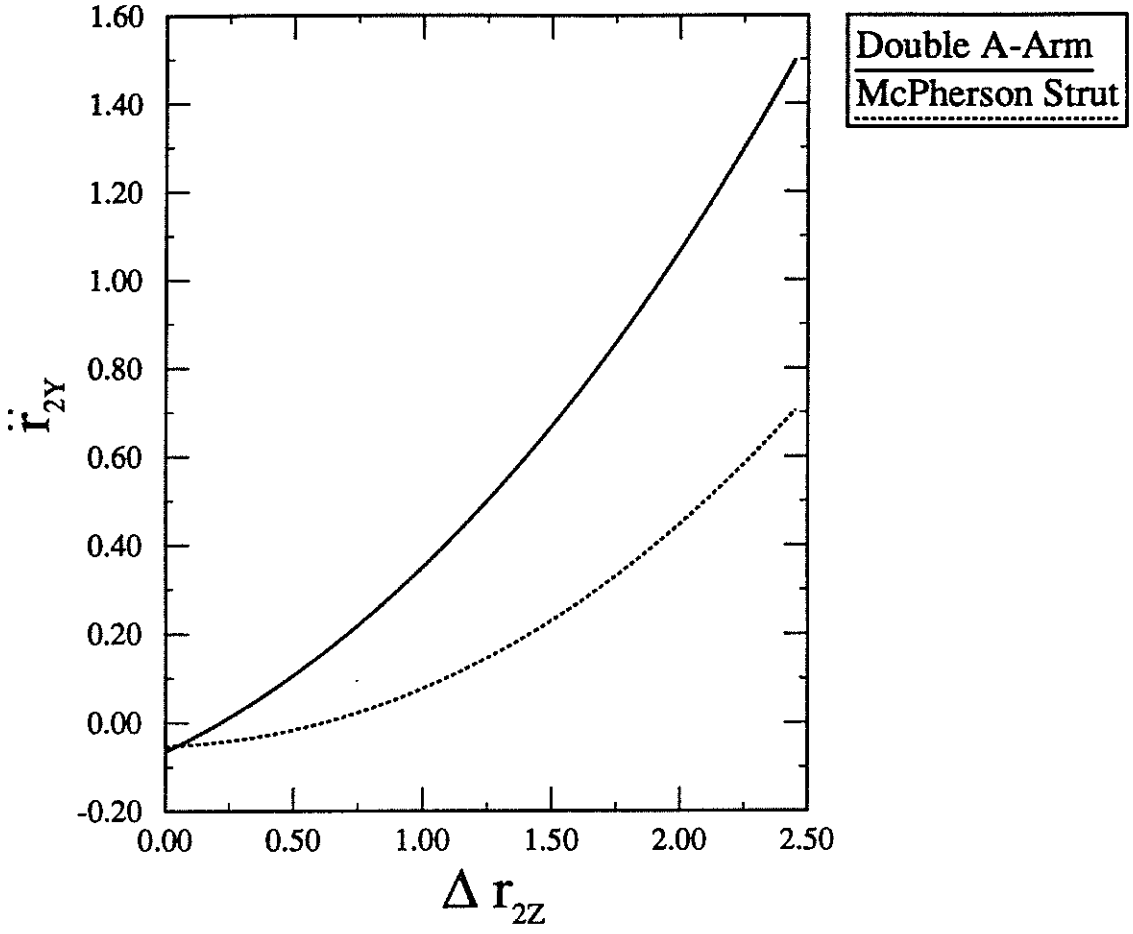

Figure 15: The linear acceleration of the tire contact point, $\ddot{r}_{2Y}$ versus the relative displacement in the Z-direction. The road is sinusodial with $A_0 = 2.5$ inches, $\lambda = 20$ feet, $\dot{X} = 88$ ft/sec. and $\ddot{X} = 0.0$.

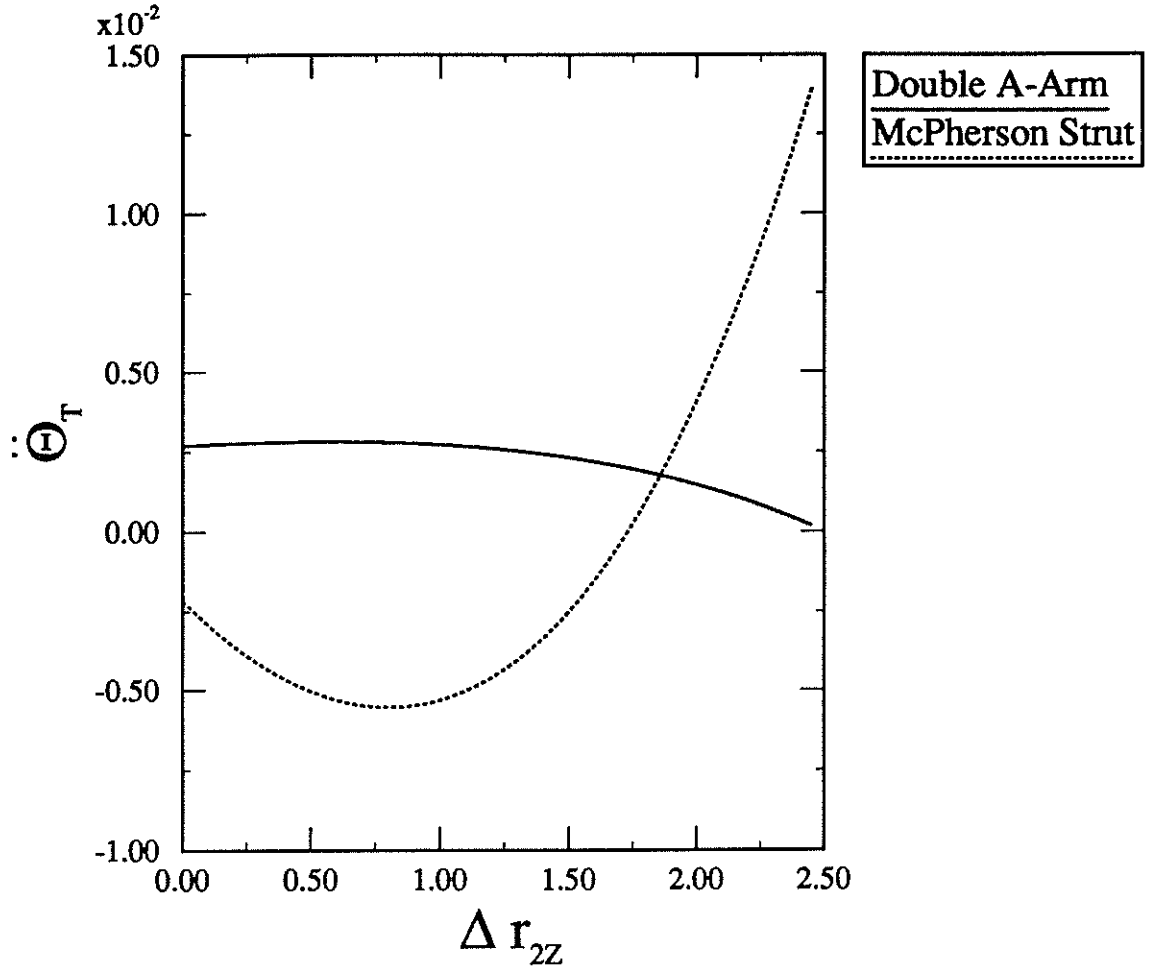

Figure 20: The angular acceleration of the spindle, $\ddot{\theta}_T$ versus the relative displacement in the Z-direction. The road is sinusodial with $A_0 = 2.5$ inches, $\lambda = 20$ feet, $\dot{X} = 88$ ft/sec. and $\ddot{X} = 0.0$.

BIBLIOGRAPHY

Allen, R. W., Rosental, T. J., and Szostak, H. T., "Steady State and Transient Analysis of Ground Vehicle Handling," SAE Paper 870495, 1987.

Allen, R. W., Szostak, H. T., Rosental, T. J., and Johnston, D. E., "Test Methods and Computer Modeling for the Analysis of Ground Vehicle Handling," SAE Paper 861115, 1986.

Anderson, D.O., L.K. Guice, "Traffic Accident Simulation Using Interactive Computer Graphics," LTRC Final Report, 1991.

Bell, S. S., Garrot, W. R., Ellis, J. R. and Liao, Y. C., "Suspension Testing Using the Suspension Parameter Measurement Device," SAE Paper 870577, 1987.

Bergman, W.,"The Basic Nature of Vehicle Understeer-Oversteer," SAE Paper 975B,1965.

Black, R. J.,"Comments on "Synthesis of Tire Equations for Use in Shimmy and Other Dynamic Studies," Journal of Aircraft, Vol. 9, No. 4, 1972.

Bundorf, R. T.,"The Influence of Vehicle Design Parameters on Characteristic Speed and Understeer,"SAE Paper 670078, 1967.

Clark, S. K., Dodge, R. N., Lackey, J. I. and Nybakken, G. H.,"Structural Modeling of Aircraft Tires," Journal of Aircraft, Vol. 9, No. 2, 1972.

Clark, S. K., Dodge, R. N. and Nybakken, G. H.,"Dynamic Properties of Aircraft Tires," Journal of Aircraft, Vol. 11, No. 3, 1974.

Ellis, J. R.,"Vehicle Dynamics," London Business Books Limited, London, 1969

Ellis, J. R., Burns, S. C., Garrott, W. R. and Bell, S. C., "The Design of a Suspension Parameter Measurement Device," SAE Paper 870576, 1987.

Ellis, J. R., "Road Vehicle Dynamics," John R. Ellis, Inc., Akron, Ohio, 1988. Garrott, W. R., Monk, M. W. and Chrstos, J. P.," Vehicle Inertial Parameters- Measured Values and Approximations," SAE Paper 881767, 1988.

Hall, A.S., "Notes on Mechanism Analysis," Waveland Press 1981.

Haug, E. J.,"Computer Aided Kinematics and Dynamics of Mechanical Systems," Allyn and Bacon,Needham Heights, MA, 1989.

APPENDIX

The following four equations that describe the position of the links of the double a-arm are not linear therefore Newton's method was used to reduce them to sets of four linear equations as shown in the matrix representation in Equation 23.

$$\begin{aligned}
\sum Y_1 &= r_Z \cos\theta_Z + r_{F1}\cos\theta_{F1} + r_{LA}\cos\theta_{LA} + r_C\cos(\theta_{KP}-\alpha) - r_{2Z}\cos\theta_{2Z} - r_{2Y}\cos\theta_{2Y} = 0 \approx \epsilon_1 \\
\sum Z_1 &= r_Z \sin\theta_Z + r_{F1}\sin\theta_{F1} + r_{LA}\sin\theta_{LA} + r_C\sin(\theta_{KP}-\alpha) - r_{2Z}\sin\theta_{2Z} - r_{2Y}\sin\theta_{2Y} = 0 \approx \epsilon_2 \\
\sum Y_2 &= r_{LA}\cos\theta_{LA} + r_{KP}\cos\theta_{KP} - r_{UA}\cos\theta_{UA} - r_{F2}\cos\theta_{F2} = 0 \approx \epsilon_3 \\
\sum Z_2 &= r_{LA}\sin\theta_{LA} + r_{KP}\sin\theta_{KP} - r_{UA}\sin\theta_{UA} - r_{F2}\sin\theta_{F2} = 0 \approx \epsilon_4
\end{aligned} \tag{22}$$

The "linearized" positions for the double a-arm are

$$\begin{Bmatrix} -\epsilon_1 \\ -\epsilon_2 \\ -\epsilon_3 \\ -\epsilon_4 \end{Bmatrix} = \begin{bmatrix} -r_{LA}\sin\theta_{LA} & , -r_C\sin(\theta_{KP}-\alpha) & , 0 & 1 \\ -r_{LA}\cos\theta_{LA} & , -r_C\cos(\theta_{KP}-\alpha) & , 0 & 0 \\ -r_{LA}\sin\theta_{LA} & , -r_{KP}\sin\theta_{KP} & , r_{UA}\sin\theta_{UA} & 0 \\ r_{LA}\cos\theta_{LA} & , r_{KP}\cos\theta_{KP} & , -r_{UA}\cos\theta_{UA} & 0 \end{bmatrix} \begin{Bmatrix} \Delta_{LA} \\ \Delta_{KP} \\ \Delta_{UA} \\ \Delta_{r_{2Y}} \end{Bmatrix} \tag{23}$$

Likewise, the following four equations that describe the positions of the links of the McPherson strut are not linear. In the same manner, they were also linearized as shown in Equation 25.

$$\begin{aligned}
\sum Y_1 &= r_Z \cos\theta_Z + r_{F1}\cos\theta_{F1} + r_{LA}\cos\theta_{LA} + r_C\cos(\theta_S-\alpha) - r_{2Z}\cos\theta_{2Z} - r_{2Y}\cos\theta_{2Y} = 0 \approx \epsilon_1 \\
\sum Z_1 &= r_Z \sin\theta_Z + r_{F1}\sin\theta_{F1} + r_{LA}\sin\theta_{LA} + r_C\sin(\theta_S-\alpha) - r_{2Z}\sin\theta_{2Z} - r_{2Y}\sin\theta_{2Y} = 0 \approx \epsilon_2 \\
\sum Y_2 &= r_{LA}\cos\theta_{LA} + r_P\cos(\theta_S-90) + r_S\cos\theta_S - r_{F2}\cos\theta_{F2} = 0 \approx \epsilon_3 \\
\sum Z_2 &= r_{LA}\sin\theta_{LA} + r_KP\sin(\theta_S-90) + r_S\sin\theta_S - r_{F2}\sin\theta_{F2} = 0 \approx \epsilon_4
\end{aligned} \tag{24}$$

$$\begin{Bmatrix} -\epsilon_1 \\ -\epsilon_2 \\ -\epsilon_3 \\ -\epsilon_4 \end{Bmatrix} = \begin{bmatrix} -r_{LA}\sin\theta_{LA} & , -r_C\sin(\theta_S-\alpha) & , 0 & 1 \\ -r_{LA}\cos\theta_{LA} & , -r_C\cos(\theta_S-\alpha) & , 0 & 0 \\ -r_{LA}\sin\theta_{LA} & , -r_P\sin(\theta_S-90) - r_S\sin\theta_S & , \cos\theta_S & 0 \\ r_{LA}\cos\theta_{LA} & , r_P\cos(\theta_S-90) - r_S\cos\theta_S & , \sin\theta_S & 0 \end{bmatrix} \begin{Bmatrix} \Delta_{LA} \\ \Delta_{KP} \\ \Delta_{r_S} \\ \Delta_{r_{2Y}} \end{Bmatrix} \tag{25}$$

Both [4 x 4] linear equations were solved using Gauss Elimination techniques.

This public document is published at a total cost of $ 702.91 . One Hundred and Seventy Five (175) copies of this public document were published in this first printing at a cost of $ 507.91 . The total cost of all printings of this document including reprints is $ 702.91 . This document was published by Louisiana State University, Graphic Services, 3555 River Road, Baton Rouge, Louisiana 70802, to report and publish research findings of the Louisiana Transportation Research Center as required in R.S.48:105. This material was printed in accordance with standards for printing by State Agencies established pursuant to R.S.43:31. Printing of this material was purchased in accordance with the provisions of Title 43 of the Louisiana Revised Statutes.